BRAIN
A JOURNAL OF NEUROLOGY

Eliciting inflammation enables successful rehabilitative training in chronic spinal cord injury

Abel Torres-Espín,[1,2] Juan Forero,[1,2] Keith K. Fenrich,[1,2] Ana M. Lucas-Osma,[1,2] Aleksandra Krajacic,[1,2] Emma Schmidt,[1,2] Romana Vavrek,[1,2] Pamela Raposo,[1,2] David J. Bennett,[1,2] Phillip G. Popovich[3] and Karim Fouad[1,2]

See Spejo and Moon (doi:10.1093/brain/awy148) for a scientific commentary on this article.

Rehabilitative training is one of the most successful therapies to promote motor recovery after spinal cord injury, especially when applied early after injury. Polytrauma and management of other medical complications in the acute post-injury setting often preclude or complicate early rehabilitation. Therefore, interventions that reopen a window of opportunity for effective motor training after chronic injury would have significant therapeutic value. Here, we tested whether this could be achieved in rats with chronic (8 weeks) dorsolateral quadrant sections of the cervical spinal cord (C4) by inducing mild neuroinflammation. We found that systemic injection of a low dose of lipopolysaccharide improved the efficacy of rehabilitative training on forelimb function, as assessed using a single pellet reaching and grasping task. This enhanced recovery was found to be dependent on the training intensity, where a high-intensity paradigm induced the biggest improvements. Importantly, in contrast to training alone, the combination of systemic lipopolysaccharide and high-intensity training restored original function (reparative plasticity) rather than enhancing new motor strategies (compensatory plasticity). Accordingly, electrophysiological and tract-tracing studies demonstrated a recovery in the cortical drive to the affected forelimb muscles and a restructuration of the corticospinal innervation of the cervical spinal cord. Thus, we propose that techniques that can elicit mild neuroinflammation may be used to enhance the efficacy of rehabilitative training after chronic spinal cord injury.

1 Faculty of Rehabilitation Medicine, University of Alberta; Edmonton, Alberta, Canada
2 Neuroscience and Mental Health Institute, University of Alberta; Edmonton, Alberta, Canada
3 Center for Brain and Spinal Cord Repair, Department of Neuroscience, 460 W. 12th Ave., 694 Biomedical Research Tower, Ohio State University; Columbus, Ohio, 43210, USA

Correspondence to: Karim Fouad
Faculty of Rehabilitation Medicine, 3-48 Corbett Hall, University of Alberta; Edmonton
Alberta, Canada, T6G 2G4
E-mail: karim.fouad@ualberta.ca

Introduction

Spinal cord injury is a devastating event causing permanent loss of motor, sensory and autonomic functions below the level of the injury. Currently, rehabilitative motor training is one of the most effective and reliable approaches to promote motor recovery after incomplete spinal cord injury (Harkema *et al.*, 2012; Nam *et al.*, 2017). Still, there are tremendous gaps in our knowledge regarding the general applicability of motor training, including the choice of training strategies and the optimal time frame for beginning training. In general, CNS injuries increase the adaptive capacity of spared neural circuits, creating a finite period in which training can effectively harness plasticity to improve functional recovery (Fouad *et al.*, 2011). Accordingly, data from individuals and animal models with stroke and spinal cord injury suggest that training efficacy diminishes when training is initiated chronically after the insult (Biernaskie *et al.*, 2004; Maulden *et al.*, 2005; Norrie *et al.*, 2005). Many factors likely contribute to this time-dependent reduction in neural plasticity but a role for neuroinflammation has not been considered as a modifier of rehabilitative training efficacy.

Inflammation after CNS injury is a complex process contributing to both tissue injury and repair (Schwartz *et al.*, 1999; Chen *et al.*, 2008; Donnelly and Popovich, 2008; Alexander and Popovich, 2009), including axon regeneration and sprouting (Yin *et al.*, 2003; Hossain-Ibrahim *et al.*, 2006; Gensel *et al.*, 2009). However, the ability to co-opt the pro-regenerative potential of neuroinflammation may be time-dependent and require selective activation or silencing of distinct receptors on immune cells (Gensel *et al.*, 2012, 2015; Kigerl *et al.*, 2014; Freria *et al.*, 2017). As an example, Shine and colleagues showed that viral-mediated overexpression of neurotrophin 3 (NT-3) in motor neurons below the level of a corticospinal tract lesion, enhanced plasticity and sprouting in spared corticospinal axons, but only if NT-3 was expressed within 2 weeks after injury (Chen *et al.*, 2006). Indeed, by 4 months post-injury, viral-mediated overexpression of NT-3 was not able to elicit growth/plasticity in uninjured corticospinal axons unless inflammation was induced by systemic injection of lipopolysaccharide (LPS) (Chen *et al.*, 2008). These data suggest that components of the early inflammatory response after injury can enhance plasticity within injured or intact CNS axons. Therefore, we hypothesized that reintroducing inflammation after chronic spinal cord injury will reopen a period of plasticity during which the efficacy of motor training is enhanced. Here, we tested this hypothesis by inducing a mild neuroinflammation in chronic spinal cord injured rats (8 weeks after cervical injury when training efficacy has declined; Norrie *et al.*, 2005; Wang *et al.*, 2011) using systemic injection of LPS combined with training in a reaching and grasping task.

Materials and methods

Experimental design

Animals

Adult female Lewis rats ($n = 132$, Charles River, 200–250 g) were group-housed and received water *ad libitum*. Food was restricted to 10 g a day per rat during training periods, otherwise animals had *ad libitum* access. The study was approved by a local animal care and use committee (Health Sciences) at the University of Alberta and complies with the guidelines of the Canadian Council for Animal Care.

Experiments

For the LPS dose response, 12 animals were divided in four groups [$n = 3$ per group, saline, 0.25, 0.5 or 1 mg/kg of LPS i.p. (intraperitoneal), Supplementary Fig. 1]. For training experiments, three exclusion criteria were established: (i) animals that could not learn the single pellet reaching and grasping (SPG) task properly, by doing only a few number of attempts or with a pre-injury success rate under 20%; (ii) animals with a lesion size above 35% (see histological analysis), incapacitating them to retrain after injury; and (iii) animals that did not show a reduction in the SPG task performance after injury. A resampling method was conducted to assign animals into treatment group, minimizing the average of the baseline pre-injury SPG success rate and the first available post-injury SPG measure between groups. For low-intensity training, 40 animals were originally in the experiment, seven were excluded. Thirty-three animals were divided in four groups [Saline $n = 9$, LPS $n = 9$, Saline+training (TR) $n = 8$, LPS+TR $n = 7$]. For medium-intensity training, 30 animals were originally in the experiment, nine were excluded. Twenty-one animals were finally included (LPS $n = 8$, Saline+TR $n = 6$ and LPS+TR $n = 7$). For high-intensity training, 36 animals were originally in the experiment, four were excluded. Thirty-two were finally divided in four groups (Saline $n = 9$, LPS $n = 7$, Saline+TR $n = 8$, LPS+TR $n = 8$). For technical problems, electrophysiological testing of the Saline group in high-intensity training was conducted in two different batches (four animals from the original experiment plus five new animals that only contributed to electrophysiology). The rest of the data are from the nine original animals. For the electrophysiological testing in intact animals, five rats were used. For the LPS-FITC (lipopolysaccharide-fluorescein isothiocyanate) experiments, six animals with spinal cord injury were used from the excluded animals in the training experiments (1 h after LPS-FITC $n = 3$, 6 h after LPS-FITC $n = 2$ and 1 h after LPS $n = 1$), and four intact animals were added (30 min, 1 h and 6 h after LPS-FITC, $n = 1$, $n = 1$ and $n = 2$, respectively). Each experiment was conducted once. For data collection, animal performance was video recorded and analysed without revealing the animal identifier after the analysis was done. In histology measures, a blinded researcher performed the data collection and a different researcher did the analysis.

Single pellet reaching and grasping task

Single pellet reaching and grasping task and training

The SPG enclosures, the pellet dispenser, preferred paw determination and the training protocols used in this study have been described previously (Torres-Espín *et al.*, 2018). The training protocols were manual training using single-window enclosures in low-intensity training; manual training using dual-window cages in medium-intensity training; and motorized training using dispensers attached to dual-window cages in high-intensity training. For the manual training, animals were placed into the back of the enclosure and a pellet was presented. Once the rat had completed a grasp attempt, the trainer waited until the rat moved to the back of the enclosure. Then, a new pellet was placed on the shelf and the process was repeated for the entire session. Training using dual-window enclosures (manual or dispenser) followed the same protocol described above, but pellets were placed on the shelf on the other side to encourage rats to move from one window to another (pellet holder when using dispensers). Independently of the training protocol, training was delivered for 10 consecutive minutes per session and animal, for four to five sessions a week. Training was delivered for 10 consecutive minutes per training session and animal. Training intensity was set by varying the training protocol (Fig. 1A) to change number of pellets presented in each experiment [pre-injury mean ± standard error of the pre-injury 10-min training session mean (SEM) of 18.3 ± 0.8, 48.3 ± 3.3, and 92.2 ± 4.3, for low-, medium- and high- intensity training, respectively; Fig. 1]. The experiments were conducted as follows: animals were pretrained in the SPG task for 3–4 weeks and the baseline was determined. The injury was then conducted. In medium and high intensity training a post-injury baseline was measured (1 month after spinal cord injury). After 8 weeks, animals received intraperitoneal injections of LPS/saline and the training started for those animals in the training groups. A waiting period of 8 weeks was chosen based on reports where rehabilitative training efficacy in rats declined between 4 to 12 weeks after injury (Norrie *et al.*, 2005; Wang *et al.*, 2011) and on findings that post spinal cord injury neuroinflammation had shifted compared to acute/subacute stages (Donnelly and Popovich, 2008). After 7 to 8 weeks of training (or resting) the final assessment was conducted in all animals. The SPG performance analysis was conducted in real-time or off-line from video recordings. The parameters used in the SPG analysis were: 'attempts', defined as each time the animal advanced the paw to reach for a pellet, succeeded or not; 'reaching rate', the percentage of attempts that the rat reached the pellet; 'grasping rate', the percentage of attempts that the rat reached and grasped the pellet; and 'success rate', the percentage of attempts that the rat succeeded to reach, grasp and eat the pellet. All the percentages are calculated with respect to the total number of attempts per training session.

Single pellet reaching and grasping task movement pattern analysis

At the end of rehabilitative training in the high-intensity training experiment the pattern of movements to successfully retrieve and eat a pellet was analysed as previously described (Metz and Whishaw, 2000). Briefly, high-speed video recordings (120 fps, Panasonic, DMC-FZ200 camera; resolution of 1280×720 pixels) of three successes were independently scored and the average was calculated. For animals that showed no successful trials, we quantified trials where the pellet was successfully grasped and led to the mouth but dropped right before the animal could eat it. For each analysed trial, the performance was divided into 11 sequential movement components (Fig. 2C). Each of the 11 movements was rated in a 3-point scale: 0, movement is absent: 0.5, movement is present but abnormal; 1 movement is present and normal.

Injury and drug administration

Spinal cord injury

Rats were anaesthetized using isoflurane (2.5% in a 50:50 air:oxygen mixture) and received a dorsolateral quadrant lesion at the cervical spinal cord. Briefly, the dorsal neck was shaved and cleaned with 10% chlorhexidine digluconate (Sigma-Aldrich), the skin above vertebrae C2–C5 was incised, and the muscles above spinal C3–C4 were split. A laminectomy and a unilateral dorsolateral quadrant lesion at C4 ipsilateral to the animals' preferred paw was performed using custom-made blades. Muscle layers and skin were sutured using suture thread #5. Animals were kept on a water-heated blanket until fully awake. Immediately after surgery, 4 ml of saline were injected (subcutaneous) to rehydrate the animals. Postoperative pain was managed by subcutaneous injections of buprenorphine (0.03 mg/kg) for 1 to 2 days after surgery.

LPS and LPS-FITC administration

LPS was derived from *Escherichia coli* endotoxin (serotype 055:B5, Sigma-Aldrich). LPS and LPS-FITC (055:B5, Sigma-Aldrich) were dissolved in sterile saline (pyrogen-free 0.9% saline, Hospira) for injection. Saline or LPS was administered intraperitoneally prior to the training experiments. The effect of a single systemic LPS administration on microglia activation a week after injection was determined in a dose-response fashion (Supplementary Fig. 1). In the rehabilitative training experiments, rats received two injections of saline or LPS (Fig. 1D) (0.4 mg/kg in low-intensity training and 0.5 mg/kg in medium- and high-intensity training). The injections for all the training experiments were conducted at the onset of rehabilitative training, 8 weeks after injury, and 3 weeks later (11 weeks after injury), when LPS-induced neuroinflammation starts to decay (Qin *et al.*, 2007). In those experiment, for each LPS injection, rectal and/or skin temperature were measured before and 4 h, 1, 3 and 7–10 days after, and open field activity was measured before and 1, 3 and 7–10 days after to ensure the well-being of the animals. LPS injections induced a transient sickness behaviour (i.e. body temperature changes, anhedonia and piloerection) that lasted for no more than 3 days (Supplementary Fig. 5). In the LPS dose response experiment animals were perfused 7 days after administration. In the LPS-FITC experiment, animals were perfused 30 min, 1 h or 6 h after administration.

Non-trained behavioural tasks

Open field general activity

Animals were individually placed in the centre of an acrylic open field (100×80 cm) for 5 min in a dark room (10–15 lx).
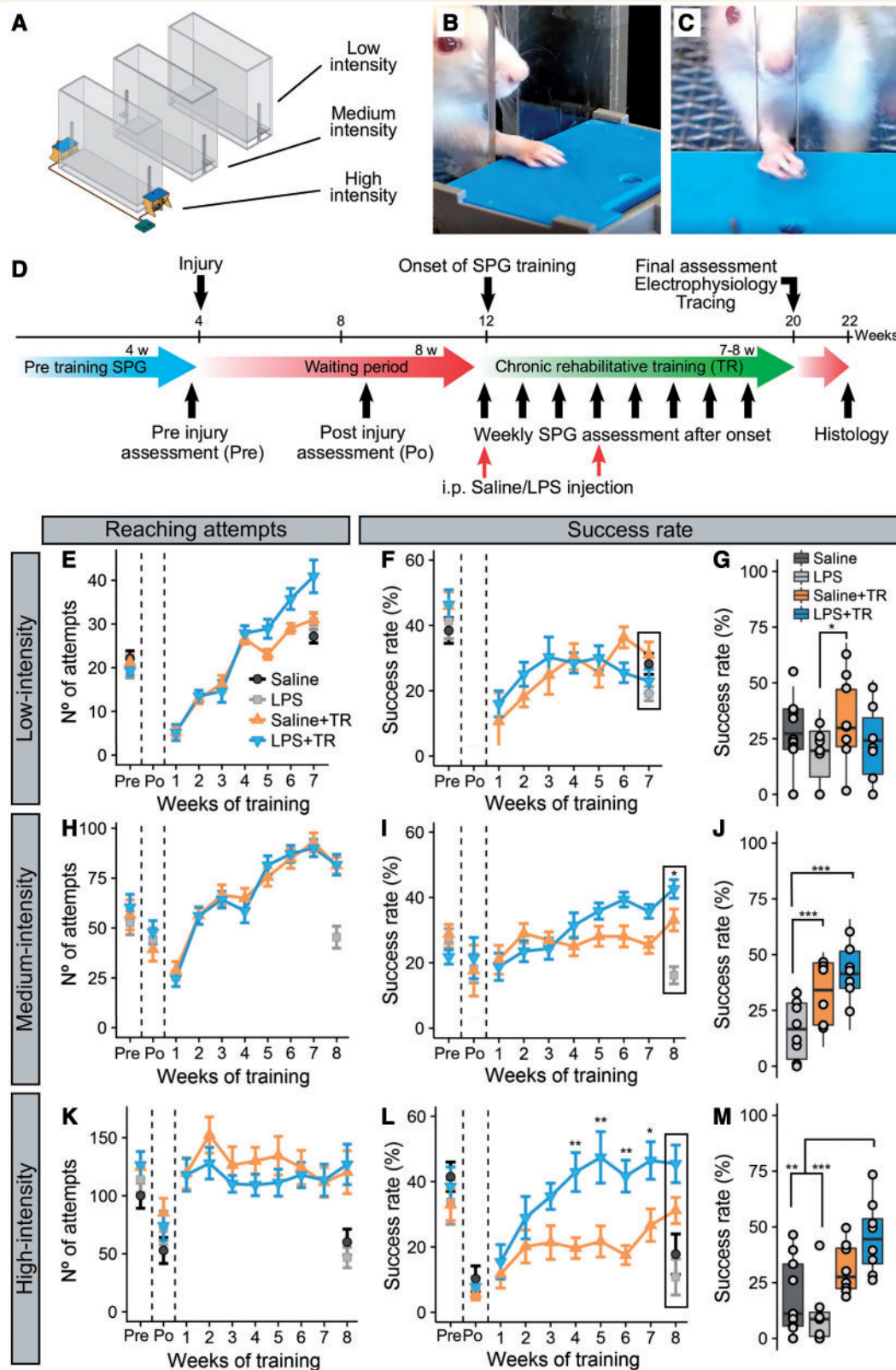
Figure 1 Systemic LPS administration improves the efficacy of high intensity motor training in rats with chronic cervical spinal cord injury. Three rehabilitative training experiments (**A**; low-, medium- and high-intensity training) were conducted using a single pellet reaching and grasping task (**B** and **C**), following the same design (**D**). For the three experiments, the weekly number of reaching attempts (**E**, **H** and **K** for low-, medium- and high-intensity training, respectively), the weekly success rate (**F**, **I** and **L** for low-, medium- and high-intensity training) and the final success rate (**G**, **J** and **M** for low-, medium- and high-intensity training) are presented. No effect of the treatment on the number of reaching attempts was observed for low- [$F(3,38.7) = 0.93$, $P = 0.435$] and medium-intensity [$F(2,18.6) = 1.02$, $P = 0.379$]. In high-

(continued)

Activity was recorded from above (Panasonic, DMC-FZ200 camera with a resolution of 1280 × 720 pixels) and analysed using custom video analysis software. The general activity was expressed as the distance animals travelled in 5 min.

Cylinder task

Rats were filmed exploring the walls of an acrylic cylinder (21 cm diameter and 25 cm high) for 5 min or at least 10 rearing movements. All wall touches of both front paws were counted. The sum of wall touches per injured paw was expressed as a percentage of the total amount of touches with both paws.

Grid walk task

Rats were filmed running in a grid walk runway (100 cm long, 12 cm wide, 12 cm high, 3 mm diameter cross bars spaced between 2 and 3 cm) with a 45° mirror underneath to capture both lateral and ventral views of the animal. Only runs with at least six consecutive steps were considered. If an animal had a misstep or slip but recovered fast enough to keep running, the run was considered as continuous. If an animal stopped, slipped, turned around or had a misstep but could not recover, the run was considered invalid and repeated. Three valid runs per animal were considered. For each paw, the number of missteps (the paw missed the targeted bar) was counted and expressed as a percentage of the total number of steps for that same paw. The average between the three videos was calculated for each animal.

Heat sensitivity plantar test

Heat sensitivity was determined using the Plantar Test Instrument (Ugo Basile). The time (in seconds) of paw withdrawal in response to infrared heat stimulus applied to the plantar surface of both forepaws was measured. A cut-off time of 20 s was set to prevent tissue damage. Five trials separated by 5 min resting periods for each forepaw were performed.

Electrophysiology

In high-intensity training, at the end of the rehabilitative training period, motor evoked potential (MEP) responses were studied in the posterior muscle compartment of both forearms. Rats were anaesthetized using ketamine/xylazine (xylazine 7 mg/kg subcutaneous, ketamine 75 mg/kg i.p.). Animals were placed in a stereotaxic frame, and a skin incision was made to expose the skull. A window over the M1 area of the forelimb motor cortex representation (0.5–1.7 mm rostral, 1–3 mm lateral to bregma) of each side was drilled with a dental drill. The stimulus was delivered by two customized tungsten monopolar electrodes mounted in the stereotaxic micromanipulator and placed transdurally 1 to 2 mm apart over the cortex. For recording in each forearm, a recording custom-made stainless-steel electrode was placed subcutaneously over the first proximal third of the posterior forearm muscle compartment, and a reference electrode was placed subcutaneously over the wrist. A subcutaneous electrode on the back served as ground. Stimuli were delivered using a stimulus generator (Master-8, A.M.P.I.) connected to a stimulus isolation unit (Isoflex, A.M.P.I.). The muscle activity was amplified (Grass P5 series a.c. pre-amplifier) and digitized at 8333 Hz (Axon instrument Digidata 1322A, 16-bit) using AxoScope software (Molecular Devices). One stimulus (0.1 ms duration) was delivered at a time. The threshold of the muscle response was determined by stimulating in the contralateral cortex of the unaffected forelimb by progressively increasing the stimulus intensity.

Figure 1 Continued

intensity training, treatment modified the number of attempts [$F_{(3,30.7)}$ = 3.9, P = 0.017], although without differences between both training groups. A significant effect of time and its interaction with treatment were observed for the three experiments [low-intensity: time effect $F_{(7,400.3)}$ = 87.79, $P < 0.001$; time × treatment effect $F_{(9,400.3)}$ = 3.65, $P < 0.001$; medium-intensity: time effect $F_{(9,461.9)}$ = 69.128, $P < 0.001$; time × treatment effect $F_{(11,461.9)}$ = , F = 3.73, $P < 0.001$; high-intensity: time effect $F_{(9,155.2)}$ = 9.015, $P < 0.001$; time × treatment effect $F_{(13,155.2)}$ = 2.81, P = 0.0012]. At any time those differences were observed between both training groups, indicating that the administration of LPS did not impact the training capacity of these animals. Regarding the success to the task, no differences between treatments were observed with the use of the low-intensity protocol [$F_{(3,35.8)}$ = 0.34, P = 0.799], and although a significant time effect [$F_{(7,400.5)}$ = 15.69, $P < 0.001$] and time-treatment interaction effect [$F_{(9,400.5)}$ = 3.85, $P < 0.001$] were found, no differences between groups were observed during the training period. At the end of the training, differences between groups were found [KWch(3) = 9.84, P = 0.02], where Saline+TR animals reached higher success rate than LPS animals (P = 0.0094). For medium-intensity experiment, no main effect of treatment was observed in the success rate [$F_{(2,21)}$ = 1.16, P = 0.33]. A time effect [$F_{(9,463.4)}$ = 5.71, $P < 0.001$] and its interaction with treatment [$F_{(11,463.4)}$ = 5.97, $P < 0.001$] were found significant. At the end of the training [$F_{(2,60)}$ = 22.98, $P < 0.001$] a significant improvement in success rate comparing Saline+TR and LPS+TR groups with LPS alone animals (P = 0.0004 and $P < 0.0001$, respectively). Moreover, an intragroup analysis showed a significant improvement of both Saline+TR and LPS+TR over time. In high-intensity experiment, a significant effect of the treatment was observed in success rate [$F_{(3,31.8)}$ = 3.9, P = 0.0176], as well as an effect of time [$F_{(9,155.6)}$ = 20.11, $P < 0.0001$] and the interaction between both [$F_{(13,155.6)}$ = 4.77, $P < 0.0001$]. Intra-group analysis of time effect showed that both Saline+TR and LPS+TR improved over time, while no improvement is observed in non-trained animals. A pairwise comparison showed differences between LPS+TR and Saline+TR groups at 4 (P = 0.0062), 5 (P = 0.002), 6 (P = 0.042) and 7 (P = 0.027) weeks after rehabilitative training onset. At the end of the rehabilitative training [$F_{(3,28)}$ = 7.61, P = 0.0007], LPS+TR animals had a significant higher success rate than both Saline and LPS alone groups (P = 0.0074 and P = 0.0007, respectively). These results indicate that rehabilitative training induce recovery when sufficient training intensity is applied. Finally, the injection of LPS enhanced the efficacy of rehabilitative training after chronic cervical spinal cord injury, especially when high-intensity training is delivered. Pre = pre-injury baseline; po = post-injury baseline. ***$P < 0.001$, **$P < 0.01$, *$P < 0.05$. In line graphs mean and SEM are represented. In box-plots median (*middle* line), first and third quartile range (box) and IQR of 1.5 (whiskers) are represented.
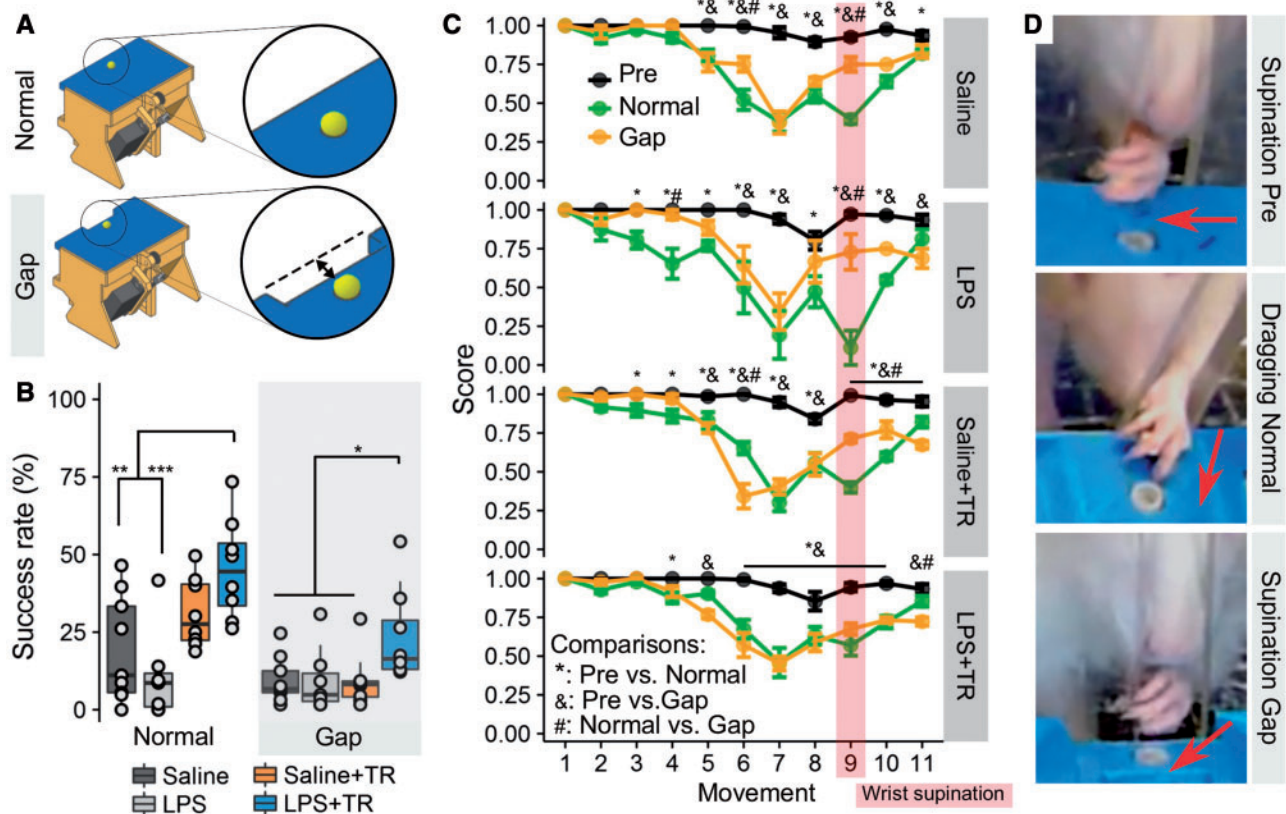
Figure 2 Systemic LPS administration and high intensity motor training reduce compensatory strategies for SPG task success. At the end of the training period, animals in high-intensity training were also tested in a modified SPG task with a 7-mm wide gap between the pellet and the slit (**A**, gap) to prevent scooping. A main effect was found between groups [KWch(3) = 9.62, $P = 0.022$]. Animals in the combined LPS+TR group showed a higher success rate in the gap SPG than the rest of the groups (versus: LPS $P = 0.019$, Saline $P = 0.016$, Saline+TR $P = 0.017$) (**B**). The movement sequence of succeeded attempts (**C**, see below) shows a change in all the animals between pre-injury (pre) and post-injury (normal and gap) assessments, independently of the group [Saline: $F(2,155.3) = 195.74$, $P < 0.0001$; Saline+TR: $F(2,164.2) = 209.89$, $P < 0.0001$; LPS: $F(2,92.8) = 108.94$, $P < 0.0001$; LPS+TR: $F(2,216.7) = 97.09$, $P < 0.0001$]. When comparing normal and gap movement sequences, differences were observed in saline (2 of 11 moves), LPS (2 of 11 moves), Saline+TR (4 of 11 moves) and LPS+TR (2 of 11 moves) groups. The major point of difference between groups was movement 9, where LPS, Saline and Saline+TR groups ($P < 0.0001$ for each) showed differences between normal and gap mode, but not group LPS+TR ($P = 0.133$). In **D**, representative frames from high-speed videos show the normal (pre-injury) wrist supination movement before the pellet is retrieved (**D**, top). After injury, scooping strategies had developed, characterized by dragging the pellets with a partial or non-existent wrist supination (**D**, middle). In the gap SPG, pellets can only be retrieved if the wrist supinates enough to lift the pellet (**D**, bottom). Arrows indicate the direction to which the palm is facing. Movement definitions extracted from Metz and Whishaw (2000) (1) Orient, the head is oriented toward the target and the snout is inserted through the slot to sniff. (2) Limb lift, the mass of body weight is shifted from the reaching forelimb to the back, and the forepaw is lifted from the floor. The hindlimbs are aligned with the body, indicating a normal base of support. (3) Digits close, the palm is partially supinated and approaches the midline of the body, the digits are semiflexed. (4) Aim, the elbow is adducted to the body midline while the digits remain positioned on the body midline. (5) Advance, the forelimb moves forward. While the body weight shifts to the front, the head and the upper body are raised to allow the forelimb to advance into the lateral body movement toward the reaching limb. (6) Digits open, the digits are opened with accompanying discrete limb movement, the palm is not fully pronated. (7) Pronation, the elbow abducts pronating the paw over the target in an arpeggio movement. (8) Grasp, the arm remains still, while the digits close and the paw is extended and raised. (9) Supination I, the paw is supinated by 90° so that it can be withdrawn through the slot. (10) Supination II, the paw is supinated so that the palm faces the mouth, and the body is in a horizontal position. (11) Release, as the rat sits back, the food pellet is released into the mouth by opening the digits. In parallel, the head and the upper body are lowered and the other paw is raised to support the preferred forelimb. In **B**: ***$P < 0.001$, **$P < 0.01$, *$P < 0.05$. In **C**: *,&,#$P < 0.05$. Mean and SEM are represented.

Then the contralateral cortex of the affected forelimb was stimulated at 0.9, 1.25, 1.5, 1.75, 2, 2.25, 2.5, 2.75, 3 and 3.25 times the determined threshold with 1-min intervals between stimuli. Recordings from AxoScope were analysed using a custom-made software (programmed in R-Shiny v1.0.5). The responses were rectified and integrated using the R package biosignalEMG (v2.0.1, Guerrero and Macias-Diaz, 2015). In intact animals ($n = 5$), EMG responses were much larger in the muscles contralateral to the stimulated cortex than ipsilateral muscles (data not shown).

Histological analysis

Tracing

Anterograde tracing with biotinylated-dextran amine (BDA; 10 000 MW, 10%, Microprobes) was performed in high-intensity training right after the electrophysiological assessment using the same set up (see above). Three injections of 1 μl BDA each were performed using a Hamilton syringe (Reno) at a depth of 1.5 mm. The skin was sutured and animals were allowed to recover as described above. Rats were perfused 2 weeks later.

Perfusion and sample cutting

Animals were euthanized by a lethal dose of pentobarbital (Euthanyl, Bimeda-MTC, Animal-Health Inc.), followed by a transcardial perfusion with saline containing 0.02 g heparin/l for 10 min. Then saline was replaced by a fixative solution of 4% formaldehyde with 5% sucrose in phosphate buffer. Brain, spinal cord and liver were harvested, post-fixed overnight in the fixative solution and transferred into a 30% sucrose (in phosphate buffer) solution for 3 days. Spinal cord tissue was cut into a C2–C3 block, and a C4 block containing the injury site and the liver was cut into 1–2-mm thick sections. Tissue was then embedded in O.C.T (Sakura Finetek) and frozen in 2-methyl-butane at −60°C. All tissue was cut in cross sections (25 μm) using a cryostat (Thermo Scientific). Spinal cords and brains were cut at −20°C and livers at −10°C. Sections were mounted onto slides (Fisherbrand, Fisher Scientific) and stored at −20°C until a staining procedure was performed.

Lesion size and tract injury assessment

The lesion extension and injured tracts were evaluated by overlapping Cresyl violet-stained (bright-field) or autofluorescence images (epifluorescence) of spinal cord sections with a schematic of a transverse cervical C4 section. The lesion was expressed as a percentage of the overall transverse section, and the amount of corticospinal or rubrospinal tract injury was expressed as a percentage of the anatomical location and size for each tract at the injury site.

Immunohistochemistry

Frozen sections were thawed for 1 h at 37°C and rehydrated by bathing in 2 × 10 min phosphate-buffered saline (PBS), followed by two washes in PBS with 0.3% Triton™ X-100 (PBS-T) for 10 min each. Then sections were incubated in blocking buffer (2% of normal donkey serum in PBS-T) for 1 h at room temperature. Afterwards, the sections were incubated overnight at 4°C or at room temperature in rabbit-anti-Iba-1 (1:750, Wako), mouse-anti-CD68 (1:500, Bio-Rad AbD Serotec), goat-anti-FITC (1:200, Abcam) antibody in blocking buffer. Slides were then washed in PBS-T (4 × 10 min) and incubated with donkey-anti-mouse/donkey-anti-rabbit/donkey-anti-goat AF555- or AF488-conjugated (1:300, Life Technology) or rabbit-anti-mouse biotinylated (for LPS-FITC staining, 1:200, Vector) antibody in blocking buffer for 2 h at room temperature. The sections were then washed in PBS (4 × 10 min). For LPS-FITC staining, the sections were incubated with streptavidin AF488 conjugated (1:200, Life Technology) in PBS 2 h at room temperature and then washed in PBS (4 × 10 min). Sections were then cover slipped with Fluoromount™ (Southern Biotech). For BDA staining,

after thawing the samples, the slides were washed in TBS (2 × 10 min) and TBS-T (TBS with 0.5% Triton™ X-100) (2 × 10 min). The samples were then incubated with streptavidin AF488 conjugated (1:200) for 2 h at room temperature in TBS-T. Finally, the slides were washed in TBS (4 × 10 min) and cover slipped with Fluoromount™.

Image analysis

Pictures were taken using an epifluorescence (Leica DM6000B, camera Leica DFC350 FX) or confocal (Leica DMi8 and TCS SP8) microscope. For the analysis of Iba-1 and BDA staining, ImageJ (National Institutes of Health, USA) was used. For Iba-1 staining in the spinal cord, positive cell bodies were counted manually or optic density was measured as the percentage of positive staining using thresholding. For BDA staining in the spinal cord, three to five sections were imaged for each animal and each analysed block (C2–C3 and C4). For each section, the number of traced axons in the dorsal corticospinal tract were quantified using the *analyse particles* function after thresholding. The BDA+ axons in the grey matter were manually traced in ImageJ. The images were all centred and aligned using the grey/white matter merging in the dorsal column as landmarks (Fig. 4B, dashed line) and the central canal (Supplementary Fig. 6, marked as point 0,0 coordinate, asterisk). The xy coordinate of each traced BDA+ pixel was extracted and saved for each image using a custom-made ImageJ macro. Heat maps for each group and each studied block were constructed, pooling together the xy coordinates of all the animals for that specific group using two-dimensional kernel density estimation implemented in the R package MASS (v7.3.47, kde2d function, Venables and Ripley, 2002). To determine the areas with higher density, DBSCAN (density-based spatial clustering of applications with noise) was conducted with the pooled xy coordinates implemented in the R package dbscan (v1.1.1, dbscan function; Hahsler and Piekenbrock, 2017). DBSCAN analysis was weighted with the frequency of each labelled pixel with respect to the number of analysed sections to account for the difference in the number of measured sections per group. The selected clusters were grouped together in five hotspots (Fig. 4 and Supplementary Fig. 6). For each hotspot and each individual section, the CST index (number of BDA+ pixels/BDA+ axons in corticospinal tract region for that section) and the density of BDA+ pixels (% of BDA+ pixels for that hotspot respect to total BDA+ pixels for that section) were calculated. The average of the CST index and pixel density of all sections per animal was calculated.

Statistical analysis

All of the statistical methods were implemented in R (version 3.2.4, R Development Core Team, 2016) using R studio (version 1.0.136, Rstudio Team, 2015). No statistical method was used for sample size calculation. The sample size was chosen based on previous experiments in the laboratory and based on the maximal number of animals we can include in training experiments without compromising the results. For statistical inference, all of the longitudinal results in training experiments were analysed by fitting a linear-mixed model using the R package lme4 (v1.1.14, Bates *et al.*, 2015) considering the animal as the random effect. Time (weeks of training), grouping variable (experimental trained group)
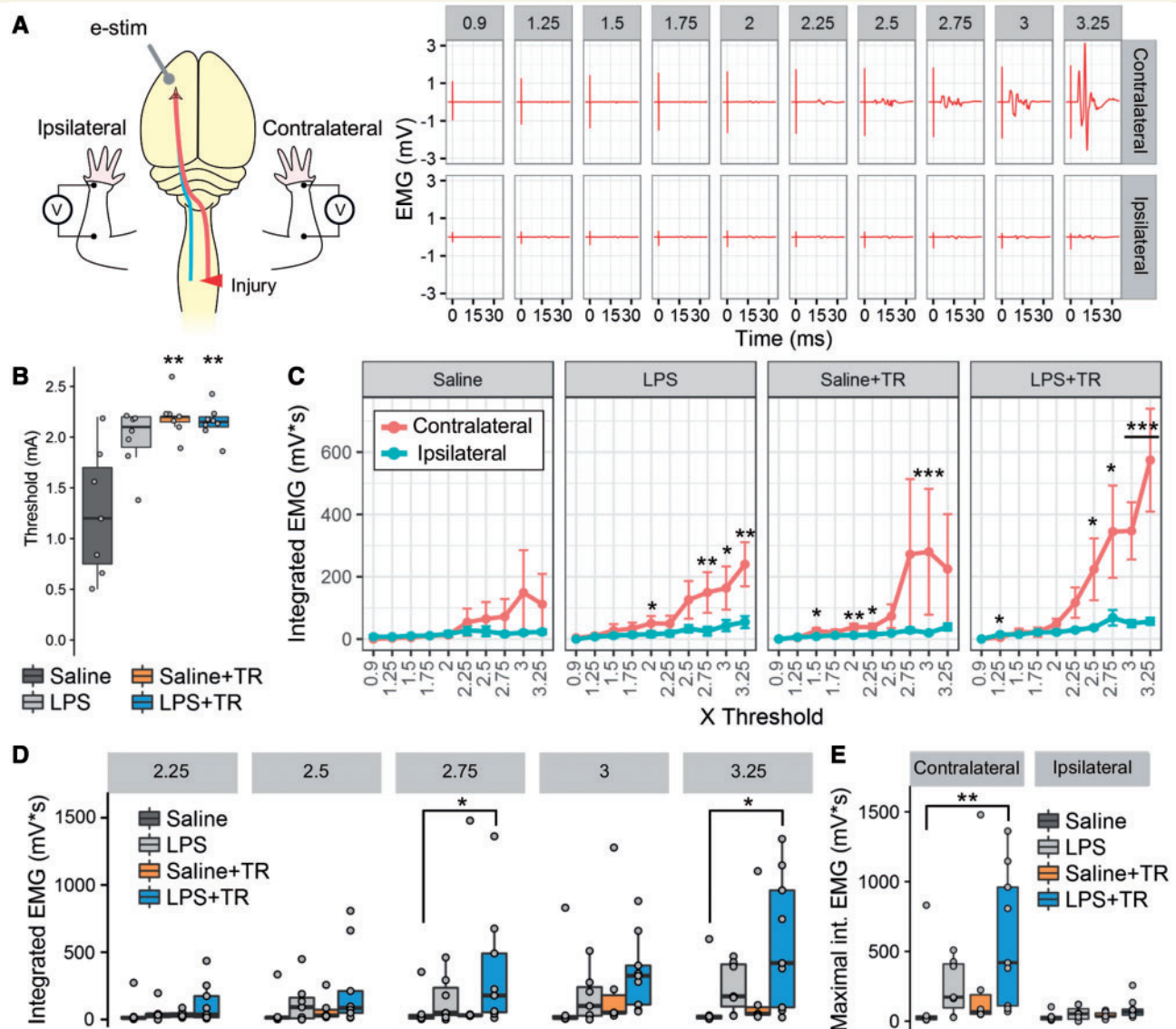
Figure 3 In combination LPS and high intensity training restore the cortical drive to forearm muscles. MEPs triggered by transdural electrical stimulation in the forelimb M1 cortical area contralateral to the operated spinal cord side were studied bilaterally in the forearm muscles (**A**). A representative MEP response is shown in **A**, with a recording for each intensity (from 0.9 to 3.25 times threshold) represented in each panel. Threshold was determined in the contralateral cortex of the unaffected arm, showing differences between groups [KWch(3) = 11.25, P = 0.01] (**B**). Threshold stimulus intensities were significantly lower in Saline animals than in Saline+TR (P = 0.002) and LPS+TR groups (P = 0.006). No differences in threshold were observed between the LPS, Saline+TR and LPS+TR groups. The integrated EMG signal was calculated and compared within (**C**) and between (**D**) groups. A significantly bigger response in the contralateral than the ipsilateral limb in LPS [$F_{(1,114)}$ = 29.36, P < 0.0001], Saline+TR [$F_{(1,95)}$ = 29.69, P < 0.0001] and LPS+TR [$F_{(1,152)}$ = 10.24, P = 0.0016], but not Saline [$F_{(1,95)}$ = 0.112, P = 0.73] groups was observed (**C**). Although no statistical difference of the group effect was found in the between groups comparison [$F_{(3,24)}$ = 1.038, P = 0.39], the interaction group × stimulus intensity was found significant [$F_{(27,216)}$ = 2.064, P = 0.0024], as well as the main effect for the stimulus intensity [$F_{(9,216)}$ = 56.71, P < 0.0001]. The MEP responses in the affected arm were similar in all the groups between 0.9 to 2.5 times threshold (**D**, only 2.25 to 3.25 times threshold are shown). At 2.75 and 3.25 times threshold, LPS+TR group showed a greater response than Saline group (P = 0.023 and P = 0.012, respectively). Moreover, the maximal MEP response in the affected arm [KWch(3) = 8.56, P = 0.035] was significantly higher (P = 0.0083) in the LPS+TR group than in the Saline group (**E**, *left*). Intermittent and small responses were detected in the unaffected arm, ipsilateral to the stimulated cortex, without differences between groups [KWch(3) = 5.36, P = 0.14] (**E**, *right*). These results are indicative of an increased cortical drive to the forearm posterior muscle compartment induced by combining LPS and training. ***P < 0.001, **P < 0.01, *P < 0.05. Data in **C** and **D** was transformed using log10(x + 1) for statistical inference using linear-mixed model. In line graphs mean and SEM are represented. In box-plots median (*middle* line), first and third quartile range (box) and IQR of 1.5 (whiskers) are represented.
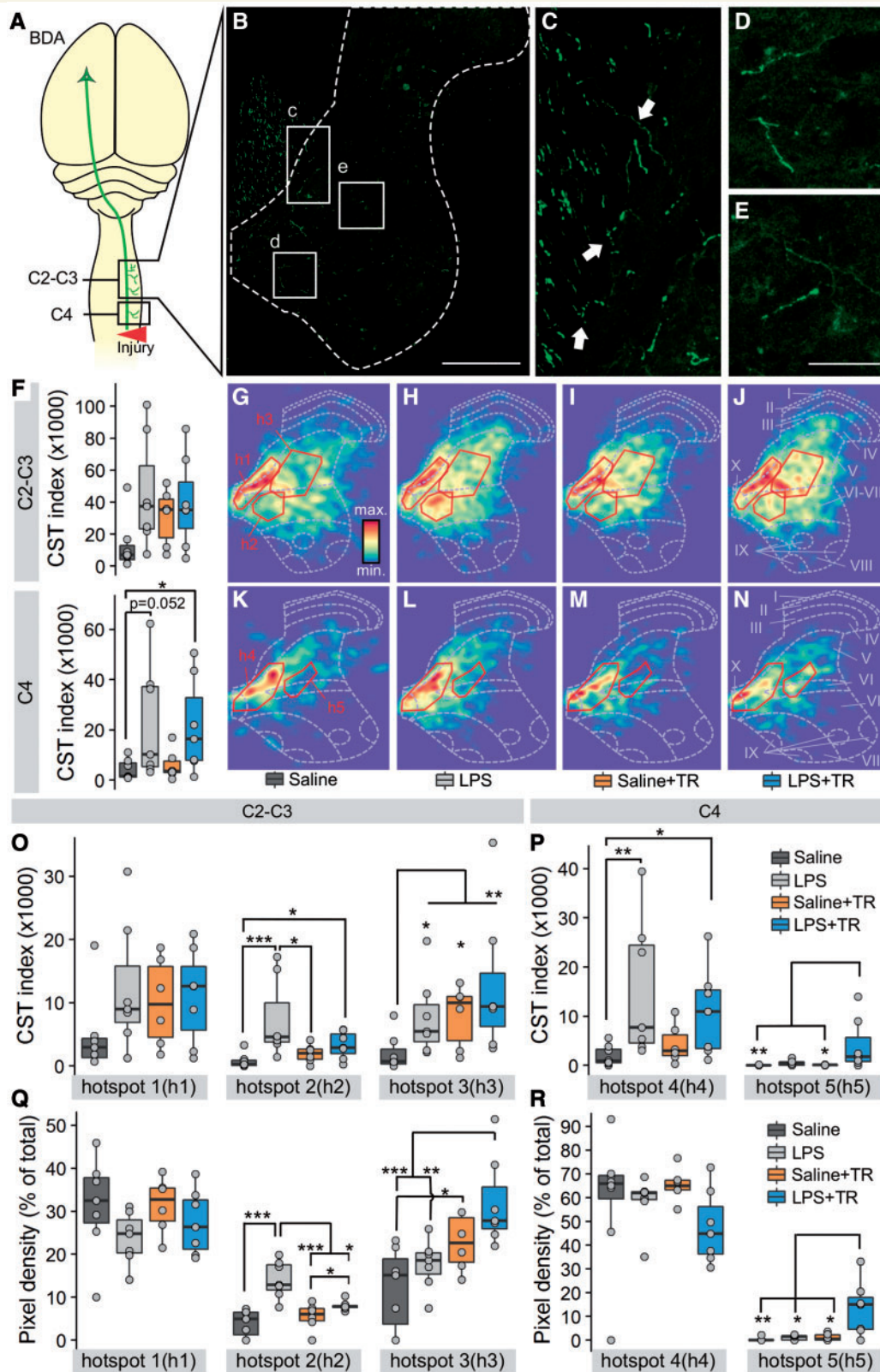
Figure 4 High intensity training, systemic LPS injections or the combination of both induce differential changes in the corticospinal tract projections above the injury site. At the end of the training period BDA was injected in the M1 forelimb cortical area. Two weeks later BDA-traced axons were counted in cross sections of the spinal cord in two blocks, C2–C3 and C4 (**A**). A representative image of the BDA+ staining for the C2–C3 region (**B**) shows the descending BDA-traced corticospinal axons in the dorsal column and their projection into the grey matter (white dotted line). Traced axons entering from the dorsal column to the grey matter (**C**, arrows) and reaching farther distances (**E** and **D**) can be appreciated. Insets **c**–**e** are expanded in **C**–**E**. The corticospinal tract index of the whole grey matter (**F**, BDA+ pixels/
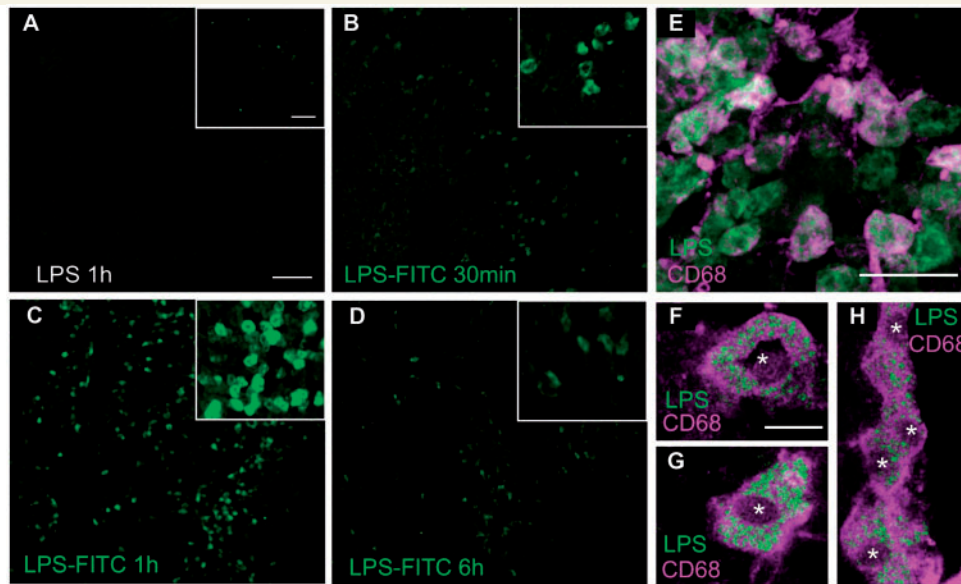
Figure 5 CD68+ cells take up LPS in the liver. LPS-FITC was systemically administered in intact and chronically injured (2 months) animals and analysed in the liver 30 min, 1 h and 6 h after injection. As a control, animals were injected with non-fluorescent LPS (**A**). LPS-FITC was already detected in the liver 30 min after injection (**B**), with a maximal presence at 1 h (**C**) and posterior reduction at 6 h after administration (**D**). A CD68 co-staining (**E**) revealed co-labelling with LPS-FITC, indicating that monocytes (phagocytic cells) are involved in the uptake of LPS. Not all LPS-FITC cells were positive for CD68, which can be explained by the fact that hepatocytes (negative for CD68) are also able to take up LPS (Deng et al., 2013). In **F** and **G** two confocal images are shown of a single CD68+ cell. LPS-FITC can be appreciated inside the cells forming granulations surrounded by CD68+ staining, present in lysosomal membranes. In **H**, an aggregation of few CD68+ cells with internalized LPS-FITC is shown. Scale bars in **A**–**D** insets = 50 μm. Scale bars in **A**–**D**: 100 μm; **E** = 50 μm; **F**–**H** = 10 μm. Asterisks indicate nuclei. See Supplementary Fig. 7 for individual channels in merged panels.

and their interaction were considered as the fixed effect. The percentage of injury, injured cortico- and rubrospinal tracts were included in the linear-mixed models to explore for possible confounding effects. A likelihood ratio test between the fitted models with and without the injury factors determined no statistical differences between models at any experiment, suggesting no statistical contribution of injury factors in the differences observed between groups. Thus, all statistical results from longitudinal data are corresponding to a linear-mixed model fitted without the injury factors. ANOVA table and P-values of the fitted linear-mixed model were generated using the *anova* function with Satterthwaite approximation of degrees of freedom from the lmerTest R package. For the analysis of all the end-point data, a one-way ANOVA

($\times$ ANOVA or a Kruskal-Wallis in the case of non-Gaussian distribution, specified in each case) was used. Multiple pairwise comparisons were performed using the R package lsmeans (v2.27.61, Lenth, 2016) adjusting the P-value by the Tukey method in the case of the linear-mixed models and one-way ANOVA. After Kruskal-Wallis, multiple pairwise comparisons were performed using Conover-Iman test of rank sum (R package conover.test v 1.1.5, Dinno, 2017) adjusting the P-value by the Holm method. An alpha value of 5% was considered as criteria for significance. All of the graphs were generated using the R package ggplot2 (v2.2., Wickham, 2009) and cowplot (v0.9.1). All measures are represented as the mean and SEM in line graphs or as the median, the first to third quartile range and 1.5 interquartile

Figure 4 Continued

number of corticospinal traced axons) was higher in LPS, Saline+TR and LPS+TR groups for C2-C3 (**F**, *top*) than Saline group without reaching statistical significance between groups [KWch(3) = 6.47, P = 0.09]. For the C4 region (**F**, *bottom*) the CST index was significantly different between groups [KWch(3) = 8.09, P = 0.044], being higher comparing the LPS+TR group with the Saline group (P = 0.042). The differences between LPS and Saline groups were close to being significant (P = 0.052). Heat maps of the BDA+ pixels in the grey matter for each group and for each analysed region were generated (**G**–**N**). A density-based spatial clustering (DBSCAN) method was used to identify highly dense regions (hotspots) in the heat maps. Five hotspots were defined (solid line insets in **G**–**N**), three in the C–C3 region (h1, h2 and h3) and two in the C4 region (h4 and h5). The CST index (**O** and **P**) represents the total amount of BDA+ pixels per traced axon for each hotspot. The pixel density (**Q** and **R**) represents the percentage of BDA+ pixels in each hotspot in respect to the total BDA+ pixels, a measure of the BDA staining distribution. In the CST index, differences between groups were found at h2 [KWch(3) = 12.78, P = 0.005], h3 [KWch(3) = 9.6, P = 0.022], h4 [KWch(3) = 10.44, P = 0.02] and h5 [KWch(3) = 10.99, P = 0.01], but not at h1 [KWch(3) = 4.12, P = 0.24]. The comparison between groups in pixel density revealed statistical differences at h2 [KWch(3) = 13.87, P < 0.0001], h3 [KWch(3) = 7.19, P = 0.001] and h5 [KWch(3) = 11.04, P = 0.011], but not at h1 [KWch(3) = 1.31, P = 0.29] nor h4 [KWch(3) = 6.04, P = 0.11]. ***P < 0.001, **P < 0.01, *P < 0.05. In box-plots median (*middle* line), first and third quartile range (box) and IQR of 1.5 (whiskers) are represented.

range (IQR) as box-plots. The statistic (i.e. F of F-test for linear-mixed models and one-way ANOVA, KWch of chi-squared for Kruskal-Wallis), the degree of freedom (in brackets after the statistic) and their probability (*P*-value) are provided in the figure legends.

Results

LPS increases the efficacy of intensive motor training in rats with chronic spinal cord injury

Eight weeks after a dorsolateral quadrant lesion at the C4 spinal cord, rats exhibit impairments in SPG tasks. At this chronic post-injury survival time, injured rats were subjected to one of three different rehabilitative SPG training intensities (high, medium or low, defined by attempt rate; see 'Materials and methods' section). Regardless of intensity, training alone did not promote significant functional recovery when compared with non-training saline treatment, although improvement overtime could be observed when medium-intensity (Fig. 1I) and high-intensity (Fig. 1L) training were applied. However, when medium-intensive training, or especially high-intensity training, was combined with systemic injections of LPS, the ability to retrieve food pellets was significantly improved. In contrast, when low-intensity training was applied, LPS significantly reduced reaching and grasping performance (Supplementary Fig. 2). Interestingly, animals that received LPS but no training showed lower reaching, grasping and retrieving performance (Fig. 1 and Supplementary Fig. 2) than all other groups. This suggests that LPS alone might be detrimental for motor recovery. The benefits of combining LPS with SPG training did not translate to non-trained tasks, including the grid walk or a vertical exploration/cylinder task (Supplementary Fig. 3).

The effects of training in combination with LPS are unlikely to be due to variability in the primary lesion, neither lesion size nor the percentage of transected cortico- and rubrospinal tracts were different between experimental groups in the high-intensity training groups (Supplementary Fig. 4). Also, since LPS-injected rats showed similar attempt rates compared to vehicle-injected rats, the mild and transient sickness response caused by LPS (Supplementary Fig. 5) did not affect the ability to train (Fig. 1E, H and K).

Despite marked effects on motor recovery, LPS, with or without training, did not affect thermal sensitivity (Supplementary Fig. 5E).

In summary, eliciting inflammatory cascades (via systemic LPS) opens a window of opportunity in which intensive training in rats with chronic spinal cord injury improves motor function. As the effects of training were most evident using the high-intensity protocol, all subsequent training experiments used this training regimen.

Combining training and LPS application reduces compensatory strategies

Rather than regaining their original motor skills, animals and individuals with CNS injuries often recover function by adopting new strategies (i.e. compensatory learning) (Alaverdashvili and Whishaw, 2013). Scooping (dragging a pellet instead of grasping and raising it) is a common strategy that rats with cervical spinal cord injury develop to retrieve pellets in the SPG task (Fenrich *et al.*, 2016). To determine whether the functional benefits of combining LPS and training are due to compensation, we introduced a gap between the pellet and the animal. This prevented the success of compensatory strategies since the pellet is lost if it is dragged (Fig. 2A and D). When such a gap was introduced, it revealed that training alone promoted compensatory function only, i.e. any benefit of training was lost when the gap was introduced. Conversely, in animals that were trained and received LPS, the functional recovery outperformed other groups despite introduction of the gap (Fig. 2B). Analysis of stereotypic movements during pellet retrieval revealed that trained animals that received LPS had closer to normal overall movement patterns with notably better wrist supination (movement 9) as compared to non-trained and trained-only groups in both normal and gap SPG task (Fig. 2C).

In conclusion, animals that were trained and injected with LPS regained grasping function by improving wrist supination and relied less on compensatory strategies.

Training and LPS increase cortically evoked motor responses in forelimb muscles

The posterior muscles of the forelimb are responsible for critical movements in the SPG task, such as wrist and digit extension, as well as supination. Given that combination of training and systemic LPS improved wrist supination, we next evaluated the cortical drive to posterior forelimb muscles (wrist and digit extensor). Specifically, we recorded MEPs following transdural electrical stimulation over the forelimb representation area of the M1 cortex, contralateral to the side of the injury. EMG recordings of the muscles were obtained bilaterally (Fig. 3A). Thresholds to elicit MEP responses were similar between LPS, training and LPS+TR animals, although these values were found to be lower in the saline, no training group when compared to the other groups (Fig. 3B). Following spinal cord injury, the MEPs in the contralateral forelimb were comparable to the ipsilateral responses in saline non-trained animals (Fig. 3C). Treated animals with either LPS, training or LPS+TR showed higher contralateral than ipsilateral EMG responses (Fig. 3C). Training alone did not significantly improve MEPs: only when combined with LPS (LPS+TR) were MEPs in affected muscles significantly increased (in comparison to MEPs in trained rats injected with saline; Fig.

3D). These data indicate that LPS and training synergize to enhance recovery of cortical drive to posterior muscles of the affected forelimb.

Training with LPS increases and directs corticospinal tract projections

To determine whether the functional (behavioural) and electrophysiological improvements noted above were associated with changes in structural plasticity, BDA was injected into the forelimb cortex contralateral to the injury side to quantify the density and distribution of corticospinal axons projecting into the cervical grey matter (Fig. 4). At C4, immediately rostral to the site of injury, training alone caused minor changes in axon density or distribution (Fig. 4F, K and M). In contrast, in rats injected with LPS, axon density increased significantly throughout grey matter (Fig. 4F, L and N). Most prominently, corticospinal axon distribution increased in more lateral grey matter regions when LPS was combined with training (Fig. 4N, P and R; see increased labelling in region h5). Note the relative absence of corticospinal axons in the h5 region at C4 in saline-injected animals.

Corticospinal axon sprouting was increased in both trained and LPS injected rats approximately two spinal segments rostral to the lesion (~C2–C3 spinal cord). Training, with or without LPS, augmented cortical innervation of the grey matter relative to spinal cord injured animals injected with saline only (no training), although without statistical significance (Fig. 4F–J). In rats injected with LPS only, many BDA+ axons were found sprouting into laminae VI and VII (Fig. 4H, O and Q; region h2), suggesting that LPS alone induces adaptive changes. The most robust effects were again noted in trained rats that received systemic LPS injections, where corticospinal axons were found sprouting deep into regions of the intermediate/lateral regions of laminae V and VI (Fig. 4J, O and Q; region h3).

In summary, when combined with our functional and electrophysiological results, these data suggest that LPS-induced neuroinflammation enhances corticospinal tract sprouting in rats with chronic spinal cord injury and that training refines this enhanced neural plasticity, creating functionally meaningful connections within spinal cord grey matter.

Systemically administered LPS bypasses the blood–spinal cord barrier only at the site of injury

Systemically administered LPS does not cross the intact blood–brain barrier (Singh and Jiang, 2004; Banks and Robinson, 2010) and since blood–spinal cord barrier integrity should be restored by 2 months post spinal cord injury (Noble and Wrathall, 1987, 1989; Popovich et al., 1996), it is unclear whether LPS acts locally within the spinal cord to improve the efficacy of rehabilitative training in rats with

chronic spinal cord injury (Fig. 1). To determine the temporal distribution of systemically injected LPS in chronically injured rats, fluorescently-labelled LPS (LPS-FITC) was injected intraperitoneally into animals 2 months after injury; then sections of liver, which quickly uptakes LPS (Scott et al., 2009), spinal cord and motor cortex were evaluated to document LPS distribution. In the liver, FITC-LPS was detected starting 30 min after injection, reaching peak levels at 1 h (Fig. 5). LPS-FITC aggregates were found inside CD68+ phagocytic macrophages (Fig. 5E–H). Consistent with previously published data, FITC staining was absent in the parenchyma of the intact spinal cord (Singh and Jiang, 2004); only trace FITC labelling existed within the lumen of large blood vessels (Fig. 6I–J). However, 2 months after spinal cord injury, modest FITC signal was observed within the injured spinal parenchyma (Fig. 6C and E–H) and, to a lesser extent, in the intact contralateral spinal cord (Fig. 6D). FITC was never detected beyond the injury site or lesion penumbra; no FITC staining was found in the spinal cord one segment rostral to the injury site (Fig. 6B) or in the cerebral cortex (Fig. 6A). At the injury site, LPS-FITC was found within CD68+ cells (Fig. 6M–O), suggesting that LPS was either phagocytosed within the injury site by microglia or transported there by monocytes that infiltrate the lesion after spinal cord injury (Popovich et al., 1999; Popovich and Hickey, 2001). These data indicate that most LPS is rapidly cleared from the blood by phagocytic hepatic macrophages (Kupffer cells) but that some circulating LPS can enter the injured spinal cord at/nearby the site of injury.

Discussion

We present new data showing that the induction of mild inflammation can enhance the efficacy of intense rehabilitative motor training in rats with chronic spinal cord injury. These effects were associated with an increase in the density of corticospinal axons sprouting into intermediate grey matter at least two to three spinal segments rostral to the site of a chronic spinal cord injury. This inflammation-induced neuroplasticity could be directed by training to form functionally meaningful connections that enhanced task-specific recovery. Importantly, this enhanced recovery was due to a restoration of lost function, limiting the use of compensatory strategies such as scooping.

Immediately after injury, the CNS enters a state of heightened plasticity when rearrangements of spared circuitry occur (Fouad and Tetzlaff, 2012), and rehabilitative training can successfully enhance this natural neuroplasticity and improve functional recovery (Girgis et al., 2007; van den Brand et al., 2012; Martinez et al., 2013). Unfortunately, this period of enhanced neuroplasticity is transient. When started in the subacute phase after injury, training is more effective in promoting functional recovery than if training is started during the chronic phase after stroke (Biernaskie et al., 2004; Maulden et al., 2005;
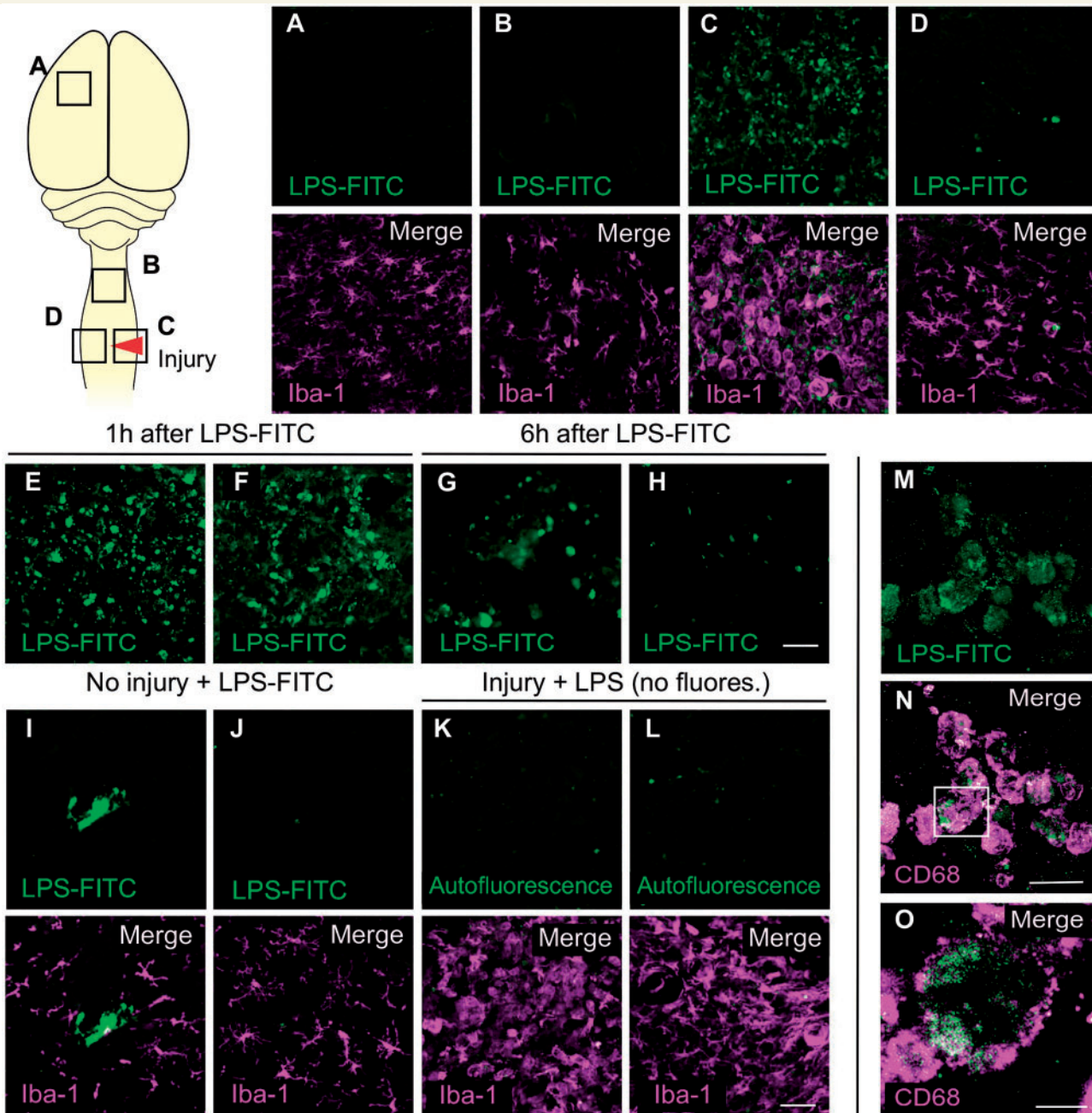
Figure 6 LPS is found in the injury site but not in intact CNS tissue after its systemic injection in chronic spinal cord injured rats. LPS-FITC was systemically administered (0.5 mg/kg i.p.) and analysed in the brain and spinal cord of non-injured and injured animals (8 weeks after injury) 1 h and 6 h after injection. Iba-1 co-staining was used to identify the injury site and areas with reactive microglial/macrophages. In the cortical motor areas (**A**) and one spinal cord segment rostral to the injury (**B**) no LPS-FITC signal was detected. Only in the injury site (**C**) and, to a lesser extent, contralateral to the injury (**D**), a positive signal for LPS-FITC was observed at 1 or 6 h after administration. Examples of two different animals for 1 h (**E** and **F**) and 6 h (**G** and **H**) after LPS-FITC injection at the injury site are shown. To demonstrate the necessity of a spinal cord injury to enable LPS-FITC to enter the cord, four intact animals were administered with tagged LPS. LPS-FITC was anecdotally localized in vessel-like structures (**I**), but never inside the spinal cord parenchyma (**J**), indicative that LPS-FITC at 0.5 mg/kg cannot enter the uninjured spinal cord. In contrast, after injury, non-fluorescent LPS was administered as a staining control. As expected, the green autofluorescence was practically non-existent in the spinal cord (**K** and **L**). Thus, the FITC+ signal found in the injury site can be attributed to the LPS-FITC presence. As observed in the liver (Fig. 5), the LPS-FITC was mainly detected inside CD68+ cells (**M–O**). A z section using confocal imaging shows the positive signal for LPS-FITC inside a CD68+ cell (**O**, inset in **N**). Scale bar in **A–I** = 100 μm; **M** and **N** = 20 μm; **O** = 10 μm. See Supplementary Fig. 7 for individual channels in merged panels.

Mazzoleni *et al.*, 2013) or spinal cord injury (Norrie *et al.*, 2005; Battistuzzo *et al.*, 2012). The exact mechanisms underlying the time-dependent decay in plasticity are unknown, although partial or complete resolution of inflammation may contribute to the finite period of enhanced plasticity. For example, the ability of NT-3 to induce sprouting of spared corticospinal axons in a model of spinal cord injury is time dependent. Sprouting can only be achieved when NT-3 is overexpressed early after injury (Chen *et al.*, 2006), but not at 4 months post-injury, unless neuroinflammation is induced via injection of LPS (Chen *et al.*, 2008). Here, we provide further evidence of inflammation-induced plasticity by showing that systemic injection of LPS alone changes corticospinal projections in the cervical grey matter months after injury. What remains unclear is how or where LPS acts to promote functionally significant neural plasticity when it is combined with training.

When injected in the periphery, most LPS is quickly cleared from the circulation in the liver (Scott *et al.*, 2009) and spleen (Groeneveld and van Rooijen, 1985) where it elicits TLR4-dependent activation of monocytes and macrophages. It is well known that LPS-induced macrophage activation initiates the synthesis and release of inflammatory cytokines including IL-1β, IL-6 and TNFα (Qin *et al.*, 2007; Hamesch *et al.*, 2015). These cytokines can enter the CNS through circumventricular organs and across the intact blood–brain barrier (Banks *et al.*, 1995). Cytokines also can initiate signal transduction and neuroinflammation through binding to receptors on endothelia and perivascular cells (Banks, 2005; Gosselin and Rivest, 2008; Serrats *et al.*, 2010; Biesmans *et al.*, 2013). This can start a neuroinflammatory process that self-perpetuates, lasting for weeks and even months after the peripheral effect of LPS has subsided (Qin *et al.*, 2007). Because systemic LPS does not cross the blood–brain barrier at the used dose (Banks, 2005), it is likely that the enhanced indices of microglia activation, that we observed in the spinal cord of LPS-injected animals were caused by these latter indirect signalling mechanisms. In addition, using FITC-labelled LPS, we did detect LPS at the injury site and nearby penumbra, suggesting that LPS could also affect plasticity by activating immune cells and glia at the injury site. Nonetheless, local injection of LPS into injured tissue, either intraocularly after an optic nerve crush injury (Baldwin *et al.*, 2015) or intraspinal after spinal cord injury (Gensel *et al.*, 2009), fails to promote axonal growth. Thus, successful induction of plasticity/axonal regeneration by systemic LPS administration may require activation of immune cells in both the CNS and peripheral organs (e.g. spleen, liver, gastrointestinal tract). However, we do not disregard the possibility that eliciting neuroinflammation by approaches that do not trigger a systemic response might be sufficient to enhance training efficacy as we report here for LPS injections. Furthermore, it is not resolved whether systemic LPS administration at multiple time points is actually required.

Although we performed a second LPS injection 3 weeks after the first one in order to counteract a possible decline in neuroinflammation (Qin *et al.*, 2007), higher doses of LPS have been reported to induce neuroinflammation as long as 10 months after systemic injection (Qin *et al.*, 2007). Future experiments are required to explore whether one injection would produce similar effects or if higher and/or longer LPS administration would provide even stronger effects on plasticity. Another unknown factor is the optimal timing between the induction of neuroinflammation and the onset of rehabilitative training. Although we could promote recovery when both were applied simultaneously, other pro-plasticity treatments were reported to be more effective in promoting recovery when combined asynchronously with training (Wahl *et al.*, 2014). Therefore, further research is necessary to determine the timing of the induced neuroinflammation to optimize the interaction with rehabilitative training.

There is increasing evidence that immune cells can influence the remodelling of neural circuitry. For instance, macrophages can promote CNS axon regeneration (Yin *et al.*, 2003; Gensel *et al.*, 2009). The activation of microglia and the recruitment of peripheral macrophages by pro-inflammatory substances such as zymosan (Gensel *et al.*, 2009) or LPS (Hossain-Ibrahim *et al.*, 2006) can increase the expression of growth factors and other proteins that induce axon sprouting. Inflammatory cytokines such as IL-1β and TNFα also enhance CREB (cAMP response element-binding) phosphorylation (Kawasaki *et al.*, 2008), which can boost neuronal activity and excitability (Galic *et al.*, 2012) and prime axonal growth (Batty *et al.*, 2017). Recent data from our group suggest that SPG efficacy and axonal sprouting (Wei *et al.*, 2016) are increased by pharmacological interventions that increase accessibility of cAMP to EPAC2 (exchange protein directly activated by cAMP). Since LPS directly or indirectly activates microglia, causing the release of inflammatory mediators that can induce cAMP in neurons (and/or glia), it is possible that the neuroinflammation induced by systemic LPS increases neuronal excitability and activates cAMP-dependent pathways along the neuroaxis (cortical and subcortical descending pathways, propriospinal interneurons, sensory afferents, etc.), prompting plasticity that can be translated to functional recovery by rehabilitative training.

The benefits of LPS were only achieved when combined with intensive training. It could be assumed that the approach described here will be beneficial for the recovery of other functions than grasping. For instance, combining LPS with treadmill training or wheel training after injuries that affect walking (such as thoracic contusions) might enhance walking recovery as we saw for grasping. That raises the question of how often preclinical treatment strategies designed to increase neuroplasticity or regeneration have been dismissed because the experimental design did not involve sufficient or any rehabilitative training. On the other hand, the mechanisms underlying spontaneous functional recovery in spinal cord injury patients are defined, in part, by

functional compensation (Curt *et al.*, 2008) rather than true recovery; i.e. recovery is driven by alternative strategies replacing the ones utilized prior to injury. Although compensatory strategies can be considered a form of motor learning, associated with neural plasticity, they might also prevent true recovery (Hylin *et al.*, 2017). To understand the potency of a treatment and to facilitate translation, it is necessary to identify the contribution of compensation to functional improvement. In our experiments, only when training was combined with LPS was a true restorative effect observed; without LPS, rats did not supinate their wrists and instead used the compensatory strategy of 'scooping' to retrieve pellets. Therefore, enhancing the malleability of the neural substrate (e.g. via induction of neuroinflammation), improves the ability of high-intensity task-specific training to promote restorative rather than compensatory motor improvements.

The combination of LPS and intensive training promoted the reorganization of corticospinal tract innervation patterns within the cervical spinal cord. In adult rats, corticospinal axons project to motor neurons via polysynaptic connections; corticospinal axons project to propriospinal neurons within intermediate laminae, prominently Rexed laminae VI and VII (Yang and Lemon, 2003; Mitchell *et al.*, 2016). In rats injected with LPS, more corticospinal tract projections distributed deeply into these laminae, indicating a possible increase in tropism to these laminae. The introduction of task-specific rehabilitation, together with LPS, modified corticospinal tract projections toward more dorsolateral areas than LPS alone, more likely laminae V and VI. Increasing projections from non-lesioned corticospinal axons to these areas has also been associated with functional recovery after stroke and forelimb rehabilitative training (Lindau *et al.*, 2014). Since LPS-induced corticospinal axon plasticity worsened motor function when training was not applied, task-specific training might be required to form meaningful connections. One should also consider the implication of other descending tracts since our injury also lesioned the rubrospinal tract and probably part of the reticulospinal tract. The rubrospinal tract is also involved in skilled reaching and grasping (Morris and Whishaw, 2016) and its reorganization after injury has been linked with recovery of forelimb function (García-Alías *et al.*, 2015; Morris and Whishaw, 2016). Nonetheless, the recovery in cortical drive to the affected muscles and the recovery of wrist supination, a function under corticospinal tract control in rats (Piecharka *et al.*, 2005), suggests cortical involvement in the improved recovery.

In conclusion, novel data in this study show that inducing mild inflammation in chronically injured spinal cord is a potential strategy to increase the efficacy of intensive rehabilitative training. Strategies like these are of vital importance to induce recovery in individuals with spinal cord injury, where limited windows of opportunity exist for introducing intensive motor training (Putman *et al.*, 2007; Granger *et al.*, 2014). These findings will likely be beneficial not only for spinal cord injuries but also for other traumatic CNS injuries and stroke.

Funding

Supplementary material

Supplementary material is available at *Brain* online.

References

Alaverdashvili M, Whishaw IQ. A behavioral method for identifying recovery and compensation: hand use in a preclinical stroke model using the single pellet reaching task. Neurosci Biobehav Rev 2013; 37: 950–67.

Alexander JK, Popovich PG. Neuroinflammation in spinal cord injury: therapeutic targets for neuroprotection and regeneration. Prog Brain Res 2009; 175: 125–37.

Baldwin KT, Carbajal KS, Segal BM, Giger RJ. Neuroinflammation triggered by β-glucan/dectin-1 signaling enables CNS axon regeneration. Proc Natl Acad Sci USA 2015; 112: 2581–6.

Banks WA. Blood-brain barrier transport of cytokines: a mechanism for neuropathology. Curr Pharm Des 2005; 11: 973–84.

Banks WA, Kastin AJ, Broadwell RD. Passage of cytokines across the blood-brain barrier. Neuroimmunomodulation 1995; 2: 241–8.

Banks WA, Robinson SM. Minimal penetration of lipopolysaccharide across the murine blood-brain barrier. Brain Behav Immun 2010; 24: 102–9.

Bates D, Mächler M, Bolker BM, Walker SC. Fitting linear mixed-effects models using lme4. J Stat Softw 2015; 67: 1–48.

Battistuzzo CR, Callister RJ, Callister R, Galea MP. A systematic review of exercise training to promote locomotor recovery in animal models of spinal cord injury. J Neurotrauma 2012; 29: 1600–13.

Batty NJ, Fenrich KK, Fouad K. The role of cAMP and its downstream targets in neurite growth in the adult nervous system. Neurosci Lett 2017; 652: 56–63.

Biernaskie J, Chernenko G, Corbett D. Efficacy of rehabilitative experience declines with time after focal ischemic brain injury. J Neurosci 2004; 24: 1245–54.

Biesmans S, Meert TF, Bouwknecht JA, Acton PD, Davoodi N, De Haes P, et al. Systemic immune activation leads to neuroinflammation and sickness behavior in mice. Mediators Inflamm 2013; 2013: 271359.

Chen Q, Smith GM, Shine HD. Immune activation is required for NT-3-induced axonal plasticity in chronic spinal cord injury. Exp Neurol 2008; 209: 497–509.

Chen Q, Zhou L, Shine HD. Expression of neurotrophin-3 promotes axonal plasticity in the acute but not chronic injured spinal cord. J Neurotrauma 2006; 23: 1254–60.

Curt A, Van Hedel HJ, Klaus D, Dietz V; EM-SCI Study Group. Recovery from a spinal cord injury: significance of compensation, neural plasticity, and repair. J Neurotrauma 2008; 25: 677–85.

Deng M, Scott MJ, Loughran P, Gibson G, Sodhi C, Watkins S, et al. Lipopolysaccharide clearance, bacterial clearance, and systemic inflammatory responses are regulated by cell type-specific functions of TLR4 during sepsis. J Immunol 2013; 190: 5152–60.

Dinno A. conover.test: Conover-Iman test of multiple comparisons using rank sums. R package version 1.1.4; 2017.

Donnelly DJ, Popovich PG. Inflammation and its role in neuroprotection, axonal regeneration and functional recovery after spinal cord injury. Exp Neurol 2008; 209: 378–88.

Fenrich KK, May Z, Torres-Espín A, Forero J, Bennetta DJ, Fouad K. Single pellet grasping following cervical spinal cord injury in adult rat using an automated full-time training robot. Behav Brain Res 2016; 299: 59–71.

Fouad K, Krajacic A, Tetzlaff W. Spinal cord injury and plasticity: opportunities and challenges. Brain Res Bull 2011; 84: 337–42.

Fouad K, Tetzlaff W. Rehabilitative training and plasticity following spinal cord injury. Exp Neurol 2012; 235: 91–9.

Freria CM, Hall JCE, Wei P, Guan Z, Mctigue DM, Phillip X, et al. Deletion of the fractalkine receptor, CX3CR1, improves endogenous repair, axon sprouting, and synaptogenesis after spinal cord injury in mice. J Neurosci 2017; 37: 3568–87.

Galic MA, Riazi K, Pittman QJ. Cytokines and brain excitability. Front Neuroendocrinol 2012; 33: 116–25.

García-Alías G, Truong K, Shah PK, Roy RR, Edgerton VR. Plasticity of subcortical pathways promote recovery of skilled hand function in rats after corticospinal and rubrospinal tract injuries. Exp Neurol 2015; 266: 112–19.

Gensel J, Nakamura S, Guan Z, van Rooijen N, Ankeny D, Popovich P. Macrophages promote axon regeneration with concurrent neurotoxicity. J Neurosci 2009; 29: 3956–68.

Gensel JC, Kigerl KA, Mandrekar-Colucci SS, Gaudet AD, Popovich PG. Achieving CNS axon regeneration by manipulating convergent neuro-immune signaling. Cell Tissue Res 2012; 349: 201–13.

Gensel JC, Wang Y, Guan Z, Beckwith KA, Braun KJ, Wei P, et al. Toll-Like receptors and dectin-1, a C-type lectin receptor, trigger divergent functions in CNS macrophages. J Neurosci 2015; 35: 9966–76.

Girgis J, Merrett D, Kirkland S, Metz GA, Verge V, Fouad K. Reaching training in rats with spinal cord injury promotes plasticity and task specific recovery. Brain 2007; 130: 2993–3003.

Gosselin D, Rivest S. MyD88 signaling in brain endothelial cells is essential for the neuronal activity and glucocorticoid release during systemic inflammation. Mol Psychiatry 2008; 13: 480–97.

Granger C, Markello S, Graham J, Deutsch A, Ottenbacher K. The uniform data system for medical rehabilitation: report of patients with stroke discharged from comprehensive medical programs in 2000-2007. Am J Phys Med Rehabil 2014; 93: 231–44.

Groeneveld PH, van Rooijen N. Localization of intravenously injected lipopolysaccharide (LPS) in the spleen of the mouse. An immunoperoxidase and histochemical study. Virchows Arch B Cell Pathol Incl Mol Pathol 1985; 48: 237–245.

Guerrero JE, Macias-Diaz JA. biosignalEMG: tools for electromyogram signals (EMG) analysis. R Packag; 2015.

Hahsler M, Piekenbrock M. dbscan: Density Based Clustering of Applications with Noise (DBSCAN) and related algorithms. R package version 1.1-1; 2017.

Hamesch K, Borkham-Kamphorst E, Strnad P, Weiskirchen R. Lipopolysaccharide-induced inflammatory liver injury in mice. Lab Anim 2015; 49: 37–46.

Harkema SJ, Schmidt-Read M, Lorenz DJ, Edgerton VR, Behrman AL. Balance and ambulation improvements in individuals with chronic incomplete spinal cord injury using locomotor training-based rehabilitation. Arch Phys Med Rehabil 2012; 93: 1508–17.

Hossain-Ibrahim MK, Rezajooi K, MacNally JK, Mason MR, Lieberman AR, Anderson PN. Effects of lipopolysaccharide-induced inflammation on expression of growth-associated genes by corticospinal neurons. BMC Neurosci 2006; 7: 8.

Hylin MJ, Kerr AL, Holden R. Understanding the mechanisms of recovery and/or compensation following injury. Neural Plast 2017; 2017: 7125057.

Kawasaki Y, Zhang L, Cheng JK, Ji RR. Cytokine mechanisms of central sensitization: distinct and overlapping role of interleukin-1beta, interleukin-6, and tumor necrosis factor-alpha in regulating synaptic and neuronal activity in the superficial spinal cord. J Neurosci 2008; 28: 5189–94.

Kigerl KA, de Rivero Vaccari JP, Dietrich WD, Popovich PG, Keane RW. Pattern recognition receptors and central nervous system repair. Exp Neurol 2014; 258: 5–16.

Lenth RV. Least-squares means: the R Package lsmeans. J Stat Softw 2016; 69: 1–33.

Lindau NT, Bänninger BJ, Gullo M, Good NA, Bachmann LC, Starkey ML, et al. Rewiring of the corticospinal tract in the adult rat after unilateral stroke and anti-Nogo-A therapy. Brain 2014; 137: 739–56.

Martinez M, Delivet-Mongrain H, Rossignol S. Treadmill training promotes spinal changes leading to locomotor recovery after partial spinal cord injury in cats. J Neurophysiol 2013; 109: 2909–22.

Maulden SA, Gassaway J, Horn SD, Smout RJ, DeJong G. Timing of initiation of rehabilitation after stroke. Arch Phys Med Rehabil 2005; 86: S34–40.

Mazzoleni S, Sale P, Tiboni M, Franceschini M, Carrozza MC, Posteraro F. Upper limb robot-assisted therapy in chronic and subacute stroke patients: a kinematic analysis. Am J Phys Med Rehabil 2013; 92: e26–37.

Metz GAS, Whishaw IQ. Skilled reaching an action pattern: stability in rat (Rattus norvegicus) grasping movements as a function of changing food pellet size. Behav Brain Res 2000; 116: 111–22.

Mitchell EJ, McCallum S, Dewar D, Maxwell DJ. Corticospinal and reticulospinal contacts on cervical commissural and long descending propriospinal neurons in the adult rat spinal cord; evidence for powerful reticulospinal connections. PLoS One 2016; 11: e0152094.

Morris R, Whishaw IQ. A proposal for a rat model of spinal cord injury featuring the rubrospinal tract and its contributions to locomotion and skilled hand movement. Front Neurosci 2016; 10: 5.

Nam KY, Kim HJ, Kwon BS, Park JW, Lee HJ, Yoo A. Robot-assisted gait training (Lokomat) improves walking function and activity in people with spinal cord injury: a systematic review. J Neuroeng Rehabil 2017; 14: 24.

Noble LJ, Wrathall JR. The blood-spinal cord barrier after injury: pattern of vascular events proximal and distal to a transection in the rat. Brain Res 1987; 424: 177–88.

Noble LJ, Wrathall JR. Distribution and time course of protein extravasation in the rat spinal cord after contusive injury. Brain Res 1989; 482: 57–66.

Norrie BA, Nevett-Ducherer JM, Gorassini MA. Reduced functional recovery by delaying motor training after spinal cord injury. J Neurophysiol 2005; 94: 255–64.

Piecharka DM, Kleim JA, Whishaw IQ. Limits on recovery in the corticospinal tract of the rat: partial lesions impair skilled reaching and the topographic representation of the forelimb in motor cortex. Brain Res Bull 2005; 66: 203–11.

Popovich PG, Guan Z, Wei P, Huitinga I, van Rooijen N, Stokes BT. Depletion of hematogenous macrophages promotes partial hindlimb recovery and neuroanatomical repair after experimental spinal cord injury. Exp Neurol 1999; 158: 351–65.

Popovich PG, Hickey WF. Bone marrow chimeric rats reveal the unique distribution of resident and recruited macrophages in the contused rat spinal cord. J Neuropathol Exp Neurol 2001; 60: 676–85.

Popovich PG, Horner PJ, Mullin BB, Stokes BT. A quantitative spatial analysis of the blood-spinal cord barrier. I. Permeability changes after experimental spinal contusion injury. Exp Neurol 1996; 142: 258–75.

Putman K, De Wit L, Schupp W, Beyens H, Dejaeger E, De Weerdt W, et al. Inpatient stroke rehabilitation: a comparative study of admission criteria to stroke rehabilitation units in four European centres. J Rehabil Med 2007; 39: 21–6.

Qin L, Wu X, Block ML, Liu Y, Breese GR, Hong J, et al. Systemic LPS causes chronic neuroinflammation and progressive neurodegeneration. 2007; 462: 453–62.

R Development Core Team. R: a language and environment for statistical computing. Vienna, Austria: R Foundation for Statistical Computing; 2016.

Rstudio Team. RStudio: integrated development for R. 2015.

Schwartz M, Moalem G, Leibowitz-Amit R, Cohen IR. Innate and adaptive immune responses can be beneficial for CNS repair. Trends Neurosci 1999; 22: 295–9.

Scott MJ, Liu S, Shapiro RA, Vodovotz Y, Billiar TR. Endotoxin uptake in mouse liver is blocked by endotoxin pretreatment through a suppressor of cytokine signaling-1-dependent mechanism. Hepatology 2009; 49: 1695–708.

Serrats J, Schiltz JC, García-Bueno B, van Rooijen N, Reyes TM, Sawchenko PE. Dual roles for perivascular macrophages in immune-to-brain signaling. Neuron 2010; 65: 94–106.

Singh AK, Jiang Y. How does peripheral lipopolysaccharide induce gene expression in the brain of rats? Toxicology 2004; 201: 197–207.

Torres-Espín A, Forero J, Schmidt E, Fouad K, Fenrich KK. A motorized pellet dispenser to deliver high intensity training of the single pellet task in rats. Behav Brain Res 2018; 336: 67–76.

van den Brand R, Heutschi J, Barraud Q, DiGiovanna J, Bartholdi K, Huerlimann M, et al. Restoring voluntary control of locomotion after paralyzing spinal cord injury. Science 2012; 336: 1182–5.

Venables WN, Ripley BD. Modern applied statistics with S. Issues of accuracy and scale. Springer; 2002. p. 868.

Wahl AS, Omlor W, Rubio JC, Chen JL, Zheng H, Schröter A, et al. Asynchronous therapy restores motor control by rewiring of the rat corticospinal tract after stroke. Science 2014; 344: 1250–5.

Wang D, Ichiyama RM, Zhao R, Andrews MR, Fawcett JW. Chondroitinase combined with rehabilitation promotes recovery of forelimb function in rats with chronic spinal cord injury. J Neurosci 2011; 31: 9332–44.Wei D, Hurd C, Galleguillos D, Singh J, Fenrich KK, Webber CA, et al. Inhibiting cortical protein kinase A in spinal cord injured rats enhances efficacy of rehabilitative training. Exp Neurol 2016; 283: 365–74.

Wickham H. ggplot2 elegant graphics for data analysis. Springer; 2009.

Yang HW, Lemon RN. An electron microscopic examination of the corticospinal projection to the cervical spinal cord in the rat: lack of evidence for cortico-motoneuronal synapses. Exp Brain Res 2003; 149: 458–69.

Yin Y, Cui Q, Li Y, Irwin N, Fischer D, Harvey AR, et al. Macrophage-derived factors stimulate optic nerve regeneration. J Neurosci 2003; 23: 2284–93.